Microwave Propagation in p-i-n Transmission Lines

Z. Zhu and A. Vander Vorst, *Fellow, IEEE*

***Abstract*—In this paper the layered structure of p-i-n photodetectors is modeled for the first time as a transmission line. The method of lines, as a two-dimensional (2-D) full-wave approach, is used to calculate the propagation constant. The numerical results agree well with measurements made on experimental devices over a frequency range of 1–30 GHz. An important new result is that the analysis of the current distribution in the bottom shielding layer shows that the finite conductivity of the high-doped semiconductor material in the layer results in a significant edge effect. This effect is properly taken into account in our 2-D model.**

***Index Terms*—Photodetectors, p-i-n, planar transmission lines.**

I. Introduction

P-I-N photodetectors are primary devices for optical carrier microwave communications systems. Microwave propagation in the p-i-n-layered structure must be evaluated for modeling p-i-n photodetectors operating at high frequencies [1]. Propagation constants of semiconductor-layered structures have been obtained by many authors [2]–[4] by using the transverse resonance method. This one-dimensional (1-D) method, however, fails to yield the correct propagation constant for the p-i-n transmission line even when the width of the transmission line is much larger than its layer thickness. This is why we used the method of lines, a two-dimensional (2-D) full-wave solution, to calculate the microwave propagation parameters in the p-i-n-layered structure. Furthermore, a set of p-i-n transmission lines was especially designed and measured to validate our simulation from 1 to 30 GHz. According to our analysis, the current in the bottom shielding layer distributes itself far beyond the strip range, due to the finite conductivity of the high-doped semiconductor material. This significant edge current is neglected by the 1-D approximation, which hence is no longer suitable for the p-i-n transmission line. This is important, since many microwave photonic devices, such as photodetectors and laser diodes, have a bottom shielding layer made of high-doped semiconductor material.

Previously, we applied the general variational method [5] to calculate the propagation parameters in the p-i-n transmission line. The results agree well with the measured ones [6]. In this letter, we use the method of lines developed by Pregla *et al.* [7], which is more efficient and accurate for the ridge structure of the p-i-n transmission lines.

Manuscript received January 10, 1997. This work was supported in part by the program Poles of Interuniversitary Attraction, Belgium State, Federal Services for Scientific, Technical, and Cultural Affairs.

The authors are with Microwave Laboratory, Université Catholique de Louvain, B-1348, Louvain-La-Neuve, Belgium.

Publisher Item Identifier S 1051-8207(97)03861-0.

II. Representation of Electromagnetic Fields in p-i-n Waveguide

The cross-sectional view of the p-i-n transmission line is shown in Fig. 1. For the ridge structure where the permittivity has an abrupt transition in the x-dimension, the longitudinal-section electric (LSE) mode Π_e and longitudinal-section magnetic (LSM) mode Π_h are convenient for describing the electromagnetic field in the waveguide [8]. They propagate along the z-direction with only one component in the x-direction, as expressed by

$$\Pi_e = \phi_e e^{\gamma z} k_o^{-2} \mathbf{a}_x \tag{1a}$$

$$\Pi_h = \phi_h e^{\gamma z} k_o^{-2} \mathbf{a}_x \tag{1b}$$

where $k_o = \omega\sqrt{\mu_o \varepsilon_o}$, $\mathbf{a}_x$ is the unit vector in the x direction and γ the propagation constant. The fields result from these modes according to

$$\mathbf{E} = \frac{1}{\varepsilon_r} \nabla \times \nabla \times \Pi_e - jk_o \nabla \times \Pi_h \tag{2a}$$

$$\mathbf{H} = jk_o \sqrt{\frac{\varepsilon_o}{\mu_o}}\, \nabla \times \Pi_e + \sqrt{\frac{\varepsilon_o}{\mu_o}}\, \nabla \times \nabla \times \Pi_h. \tag{2b}$$

The scalar potentials ϕ_h and ϕ_e must fulfill the Helmholtz equation and the Sturm–Liouville equation, respectively [8],

$$\frac{\partial^2 \phi_h}{\partial x^2} + \frac{\partial^2 \phi_h}{\partial y^2} + [\varepsilon_r(x) k_o^2 + \gamma^2]\phi_h = 0 \tag{3a}$$

$$\varepsilon_r(x) \frac{\partial}{\partial x}\left[\frac{1}{\varepsilon_r(x)} \frac{\partial \phi_e}{\partial x}\right] + \frac{\partial^2 \phi_e}{\partial y^2} + [\varepsilon_r(x) k_o^2 + \gamma^2]\phi_e = 0. \tag{3b}$$

In order to determine the boundary conditions for ϕ_h and ϕ_e, (2) shows that $\mathbf{E}_x$ is proportional to ϕ_e while $\mathbf{E}_{y,z}$ are determined by both ϕ_h and $\partial\phi_e/\partial_x$. Similarly, $\mathbf{H}_x$ is proportional to ϕ_h while $\mathbf{H}_{y,z}$ depend on both ϕ_e and $\partial\phi_e/\partial x$. Consequently, the lateral boundary conditions should be $\phi_h = 0$ and $\partial\phi_e/\partial x = 0$ for metallic walls and $\phi_e = 0$ and $\partial\phi_h/\partial x = 0$ for magnetic walls. The symmetry of the p-i-n structure requires that $\mathbf{E}_x$ of the dominant mode be zero in the middle of the strip, which corresponds to a magnetic wall locating at the middle of the strip. For mathematical convenience, an electric wall far away (500 μm) from the strip is assumed. Therefore, ϕ_e satisfies Neumann condition and Dirichlet condition on the left and right side (N–D), respectively, while ϕ_h obeys D–N boundary conditions.

To use the method of lines, the scalar potentials ϕ_e and ϕ_h are discretized by a two-line system so that they satisfy their boundary conditions individually, as shown in Fig. 1. Through adequate transformations on the discretized difference equations, the field in the transform domain is easily obtained.

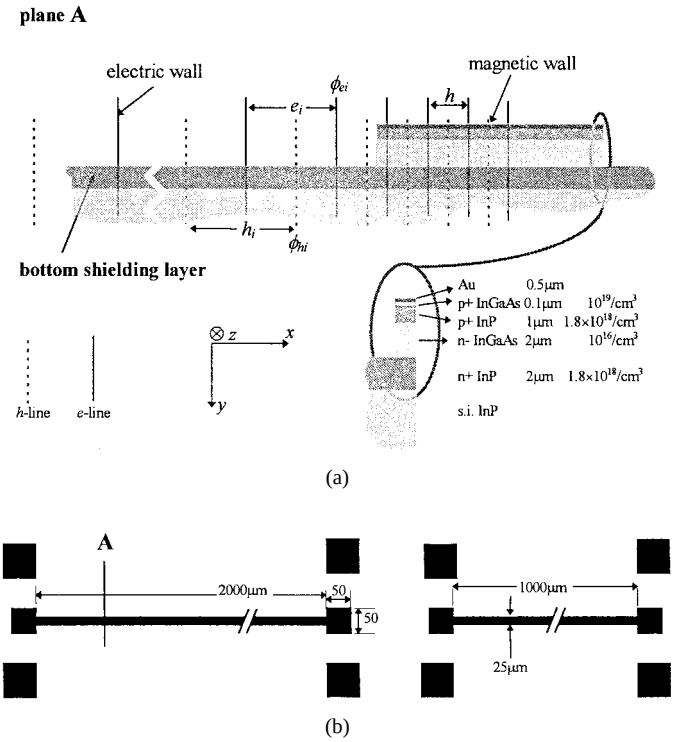

(a)

(b)

Fig. 1. P-I-N transmission lines: (a) layer structure and (b) discretization in half cross-sectional top view.

The field matching in the y-dimension is made to obtain an eigenvalue equations set from which the propagation constant and field distribution are obtained.

III. Design of p-i-n Transmission Line

The designed p-i-n transmission lines are shown in Fig. 1. The layers are grown from a semi-insulation InP substrate by organometallic vapor phase epitaxy (OMVPE) technique, which ensures a good crystal quality and an accurate thickness control. The width of the strip is 25 μm. The bonding pads for connecting the n^+ InP layer is deposited on the bottom shield layer. The thin buffer layer p^+ InGaAs is for lattice matching (this is neglected in the simulations). The doping level of the n^+ InP and p^+ InP layers is as high as possible so that the transmission lines have a low attenuation; the doping level of the n^- InGaAs absorbing layer is as low as possible to have a small depletion voltage and a uniform electric field distribution in the intrinsic layer. In the simulation, the mobilities of n^+ InP and p^+ InP materials are assigned to be 4200 and 150 $cm^2/V{\cdot}s$, respectively. Two p-i-n transmission lines with different lengths are designed for the line–line (LL) calibration and the measurements [9]. They are identical except for a uniform section ΔL, which is chosen so that the phase delay introduced by this section is between 20–160° over the whole frequency range. This is to ensure accurate measurements.

IV. Experimental Validation

Fig. 2 presents the simulated and measured results. The 1-D results are obtained with the transverse resonance method. Both the phase delay and attenuation significantly differ from

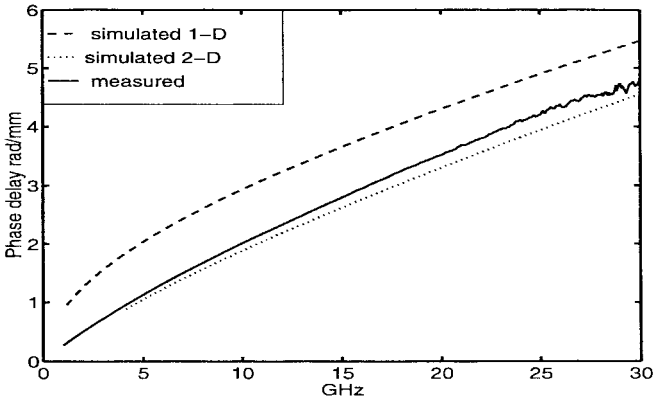

(a)

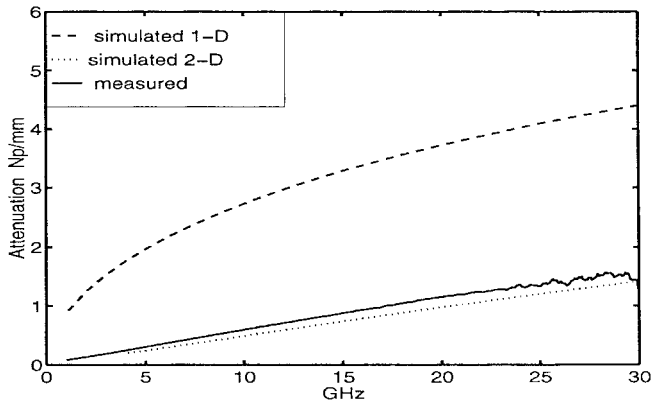

(b)

Fig. 2. Comparison of results from 1-D model, 2-D model, and measurements.

the measured results while the 2-D results agree well with the measurements. The current distribution in the bottom shielding layer is represented in Fig. 3, where it can be seen that the current distributes itself (solid curve) far beyond the width of the strip. When the bottom shielding layer (n^+ InP layer) is replaced by a gold layer, the current (dotted point) concentrates near the metal strip. As a consequence, the edge effect of the p-i-n transmission line cannot be neglected unless the bottom shielding layer is made of perfect conductor. This is why the 2-D approach is necessary. We have also developed a rapid complex root locating technique to solve the eigenvalue equations. Calculating the propagation constant at one frequency needs about 1 min for 2-D simulation and about half a second for 1-D simulation. The memory space required for 2-D simulation is about 50 times larger than for the 1-D simulation.

V. Conclusions

The 2-D full-wave solution with the method of lines was performed to obtain the propagation constant of p-i-n transmission lines. The simulated results agree well with the measured ones in a frequency range 1–30 GHz. It is shown that the 1-D approach is not valid for the p-i-n transmission line, because the current spreads over an area much larger than the width of the strip. This is an important new result. The effect is due to the finite conductivity of the bottom shielding layer.

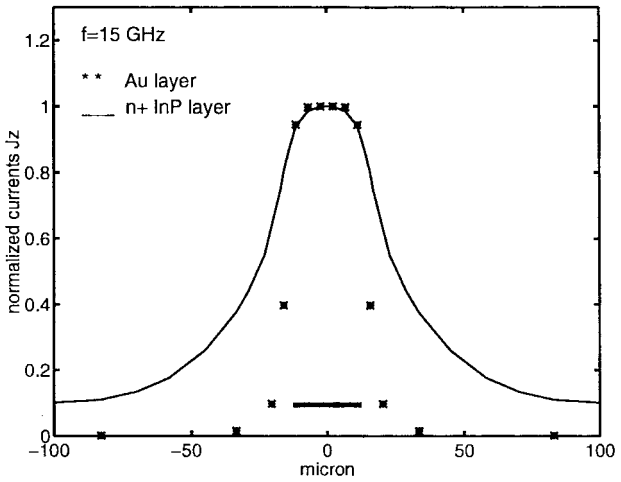

Fig. 3. Longitudinal current distribution in bottom shielding layer (long bar in middle represents metal strip, solid line is for p-i-n transmission line, and dotted points are for same structure but with n^+ InP layer replaced by gold layer).

ACKNOWLEDGMENT

The authors would like to thank Dr. I. Huynen, T. Wu, B. Stockbroeckx, and R. Gillon for fruitful discussions and help in measurements. They would also like to thank the INTEC group (University of Ghent, Belgium), which manufactured the integrated circuit.

REFERENCES

[1] Z. Zhu, R. Gillon, and A. Vander Vorst, "A new approach to broadband matching for p-i-n photodiodes," *Microwave Opt. Tech. Lett.,* vol. 8, pp. 8–13, Jan. 1995.

[2] G. H. Guckel, P. A. Brennan, and I. Palocz, "A parallel-plate waveguide approach to microminiaturized planar transmission lines for integrated circuits," *IEEE Trans. Microwave Theory Tech.,* vol. MTT-15, pp. 468–476, Aug. 1967.

[3] D. Jäger and W. Rabus, "Bias-dependent phase delay of Schottky contact microstrip line," *Electron. Lett.,* vol. 9, pp. 201–202, May 1973.

[4] I. T. Ho and S. K. Mullick, "Analysis of transmission lines on integrated circuit chips," *IEEE J. Solid-State Circuits*, vol. SC-2, pp. 201–208, Dec. 1967.

[5] I. Huynen, D. Vanhoenacker, and A. Vander Vorst, "Spectral domain form of new variational expression for very fast calculation of multilayered lossy planar line parameters," *IEEE Trans. Microwave Theory Tech.,* vol. 42, pp. 2099–2106, Nov. 1994.

[6] Z. Zhu, I. Huynen, and A. Vander Vorst, "An efficient microwave characterization of PIN photodiodes," in *Proc. 26th Euro. Microwave Conf.,* Prague, Czech Republic, Sept. 1996, pp. 1010–1014.

[7] T. Itoh, *Numerical Methods for Microwave and Millimeter Wave Passive Structures.* New York: Wiley, 1989, ch. 6.

[8] R. E. Collin, *Field Theory of Guided Wave.* New York: McGraw-Hill, 1960, ch. 6.

[9] M. Fossion, I. Huynen, D. Vanhoenacker, and A. Vander Vorst, "A new and simple calibration method for measuring planar lines parameters up to 40 GHz," in *Proc. 22nd Euro. Microwave Conf.,* Helsinki, Finland, Sept. 1992, pp. 180–185.